Cell-Centered Finite Volume Method for Regularized Mean Curvature Flow on Polyhedral Meshes

Jooyoung Hahn, Karol Mikula, Peter Frolkovič, Martin Balažovjech, and Branislav Basara

Abstract A cell-centered finite volume method is used to numerically solve a regularized mean curvature flow equation on polyhedral meshes. It is based on an over-relaxed correction method used previously for linear diffusion problems. An iterative nonlinear Crank-Nicolson method is proposed to obtain the second-order accuracy in time and space. The proposed algorithm is used for three-dimensional domains decomposed for parallel computing for two examples that numerically verify the second order accuracy on polyhedral meshes.

Keywords Regularized mean curvature flow · Polyhedral meshes · Over-relaxed correction method · Nonlinear Crank-Nicolson method

MSC (2010) 65M08 · 35G31 · 35K61

1 Introduction

A finite volume method to solve the level set formulation of regularized mean curvature flow [15] on a bounded Lipschitz continuous domain $\Omega \subset \mathbb{R}^3$ is presented:

$$\frac{\partial \phi}{\partial t} = |\nabla \phi|_\varepsilon \nabla \cdot \left(\frac{\nabla \phi}{|\nabla \phi|_\varepsilon} \right), \quad |\nabla \phi|_\varepsilon = (\varepsilon^2 + |\nabla \phi|^2)^{1/2}, \tag{1}$$

J. Hahn (✉) · B. Basara
AVL List GmbH, Hans-List-Platz 1, 8020 Graz, Austria
e-mail: jooyoung.hahn@avl.com

B. Basara
e-mail: branislav.basara@avl.com

K. Mikula · P. Frolkovič · M. Balažovjech
Department of Mathematics and Descriptive Geometry, Slovak University of Technology, Radlinskeho 11, 810 05 Bratislava, Slovakia
e-mail: karol.mikula@stuba.sk

P. Frolkovič
e-mail: peter.frolkovic@stuba.sk

R. Klöfkorn et al. (eds.), *Finite Volumes for Complex Applications IX - Methods, Theoretical Aspects, Examples*, Springer Proceedings in Mathematics & Statistics 323,
https://doi.org/10.1007/978-3-030-43651-3_72

where the regularization parameter $\varepsilon > 0$ is used as a small constant [6]. The initial and Dirichlet boundary conditions are defined by

$$\begin{aligned} \phi(\mathbf{x}, 0) &= \phi_0(\mathbf{x}), \quad \mathbf{x} \in \Omega, \\ \phi(\mathbf{x}, t) &= \phi_b(\mathbf{x}, t), \quad (\mathbf{x}, t) \in \partial\Omega \times (0, T]. \end{aligned} \tag{2}$$

The level set form of mean curvature flow equation and its modifications are extensively used in numerical applications like the filtering or segmentation in image processing [11], the G-equation in combustion models of computational fluid dynamics [16], and the interface problems in material science; see more details in [8, 14, 17] and the references therein.

To solve (1) numerically and to develop related mathematical theories, several methods are used: the finite difference [13, 17], the finite element [3], and the finite volume methods [7, 11, 19]. In this paper, a method based on a cell-centered finite volume method is proposed in order to use the smallest number of unknowns on a polyhedron mesh. For a spatial discretization, one of practically used algorithms in computer-aided engineering to discretize an elliptic operator on polyhedron meshes, so-called over-relaxed correction method, is considered [4, 12], because a formal expansion of the right-hand side of (1) is a combination of a Laplacian and a nonlinear term of second order derivatives; see more details in [18]. For a temporal discretization, a nonlinear Crank-Nicolson method [1] is considered in order to have the second order accuracy with a time step size proportional to the space discretization step. In such a way, the proposed method can be conveniently combined with second order accurate methods for an advective or normal flow equation [9, 10], e.g., for the G-equation model [16]. We also use a deferred correction method [2] in order to achieve computational efficiency with a 1-ring face neighborhood structure on domains decomposed for parallel computing.

The paper is organized as follows. In Sect. 2.1, we derive the spatial discretization based on the over-relaxed correction method. In Sect. 2.2, the iterative nonlinear Crank-Nicolson method is proposed. In Sect. 3, the experimental order of convergence for two exact solutions on two computational domains is presented.

2 Cell-Centered Finite Volume Method

The computational domain $\Omega \subset \mathbb{R}^3$ is discretized by open non-overlapping polyhedral cells Ω_p and I is the set of cell indices. We indicate a set N_p as adjacent cell indices to Ω_p, where the cells Ω_q, $q \in N_p$ have a non-zero area intersection with Ω_p. An internal face, the result of such intersection, is denoted by $e_f \subset \partial\Omega_q \cap \partial\Omega_p$ and the set of all internal faces in a mesh is denoted by F. We similarly define a set B as the index set of all boundary faces $e_b \subset \partial\Omega_p \cap \partial\Omega$ for $p \in I$. The face indices of a cell Ω_p, $p \in I$ belong either to the set $F_p \subset F$ or to the set $B_p \subset B$. A numerical solution at time t is represented by unknowns $\phi_p \approx \phi(\mathbf{x}_p, t)$, where $\mathbf{x}_p$ is the center of cell Ω_p. The Dirichlet boundary condition in (2) is evaluated at the centers $\mathbf{x}_b$ of boundary faces e_b, i.e., $\phi_b = \phi_b(\mathbf{x}_b, t)$.

We integrate (1) on $\Omega_p, p \in I$,

$$\int_{\Omega_p} \frac{1}{|\nabla\phi|_\varepsilon} \frac{\partial \phi}{\partial t} = \int_{\Omega_p} \nabla \cdot (g \nabla \phi) = \sum_{f \in F_p \cup B_p} \int_{e_f} g \nabla \phi \cdot \mathbf{n}, \tag{3}$$

where $g = |\nabla\phi_p|_\varepsilon^{-1}$, and $\mathbf{n}$ is an outward normal vector. An approximation of gradient $\nabla\phi$ on a cell Ω_p, $\nabla\phi_p \approx \nabla\phi(\mathbf{x}_p, t)$, is computed by an inverse distance weighted least-squares minimization [5, 12]:

$$\nabla\phi_p \equiv L_p(\phi_p, \phi_b) = \underset{\mathbf{y} \in \mathbb{R}^3}{\operatorname{argmin}} \left(\sum_{q \in N_p \cup B_p} |\mathbf{d}_{pq}|^{-2} (\phi_p + \mathbf{y} \cdot \mathbf{d}_{pq} - \phi_q)^2 \right). \tag{4}$$

The notation $\mathbf{d}_{\alpha\beta} \equiv \mathbf{x}_\beta - \mathbf{x}_\alpha$ for directional vectors is used throughout the paper.

In Sect. 2.1, we present a spatial discretization of (3), including an approximation of normal flux $g\nabla\phi \cdot \mathbf{n}$. Afterwards, in Sect. 2.2, we discuss a temporal discretization.

2.1 Over-Relaxed Correction Method

In a derivation of spatial discretization, we follow mostly [4, 12]. We assume that all variables are continuous at the face centers $\mathbf{x}_f, f \in F$, and we denote their values by the subscript f. For an internal face e_f, the normal flux in (3) at time t is first approximated by

$$f \in F_p \Rightarrow \int_{e_f} g \nabla\phi \cdot \mathbf{n} \approx g_f \nabla\phi_f \cdot \mathbf{n}_{pf}, \tag{5}$$

where $\mathbf{n}_{pf}$ is the outward normal vector to the face such that $|\mathbf{n}_{pf}| = |e_f|$.

We use an orthogonal decomposition of the vector $\mathbf{d}_{pq}$ with respect to $\mathbf{n}_{pf}$ and $\mathbf{t}_f$, $\mathbf{n}_{pf} \perp \mathbf{t}_f$, written formally in the form

$$\mathbf{d}_{pq} = \frac{g_f}{c_f} \mathbf{n}_{pf} - \mathbf{t}_f, \tag{6}$$

where

$$c_f = g_f \frac{\mathbf{n}_{pf} \cdot \mathbf{n}_{pf}}{\mathbf{n}_{pf} \cdot \mathbf{d}_{pq}}, \quad \mathbf{t}_f = \left(\frac{\mathbf{n}_{pf}}{|\mathbf{n}_{pf}|} \cdot \mathbf{d}_{pq} \right) \frac{\mathbf{n}_{pf}}{|\mathbf{n}_{pf}|} - \mathbf{d}_{pq}.$$

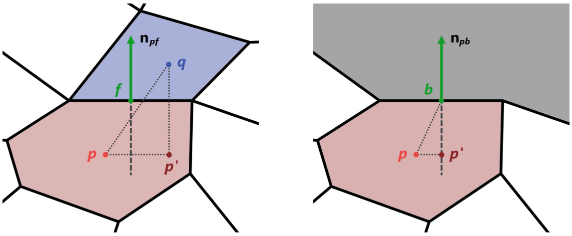

(a) (b)

Fig. 1 In **a**, the notation for an internal face $e_f, f \in F_p$ is shown, and $\mathbf{d}_{p'p} \perp \mathbf{n}_{pf}$. In **b**, the notation for a boundary face $e_b, b \in B_p$ is shown with the gray region being outside of the computational domain, and $\mathbf{d}_{p'p} \perp \mathbf{n}_{pb}$

Note that $\mathbf{t}_f = \mathbf{d}_{p'p}$ in Fig. 1a. Rewriting (6) as $g_f \mathbf{n}_{pf} = c_f(\mathbf{d}_{pq} + \mathbf{t}_f)$, we can derive the approximation:

$$g_f \nabla\phi_f \cdot \mathbf{n}_{pf} \approx c_f \left(\phi_q - \phi_p + \nabla\phi_f \cdot \mathbf{t}_f\right). \tag{7}$$

The face gradient $\nabla\phi_f$ is approximated from gradients in the adjacent cells,

$$\nabla\phi_f = \omega_{qf}\nabla\phi_p + \omega_{pf}\nabla\phi_q, \quad \omega_{pf} + \omega_{qf} = 1, \quad \omega_{pf} = \frac{|\mathbf{d}_{pf}|}{|\mathbf{d}_{pf}| + |\mathbf{d}_{qf}|}.$$

Similarly, for a boundary face, the normal flux $g\nabla\phi \cdot \mathbf{n}$ in (3) is approximated by

$$b \in B_p \Rightarrow \int_{e_b} g\nabla\phi \cdot \mathbf{n} \approx g_p \nabla\phi_p \cdot \mathbf{n}_{pb}. \tag{8}$$

Using analogous orthogonal decomposition of $\mathbf{d}_{pb}$ in Fig. 1b, and $g_p\mathbf{n}_{pb} = c_b(\mathbf{d}_{pb} + \mathbf{t}_b)$, where $\mathbf{n}_{pb} \perp \mathbf{t}_b$, it gives us a discretization:

$$g_p \nabla\phi_p \cdot \mathbf{n}_{pb} \approx c_b(\phi_b - \phi_p + \nabla\phi_p \cdot \mathbf{t}_b), \tag{9}$$

where

$$c_b = g_p \frac{\mathbf{n}_{pb} \cdot \mathbf{n}_{pb}}{\mathbf{n}_{pb} \cdot \mathbf{d}_{pb}}, \quad \mathbf{t}_b = \left(\frac{\mathbf{n}_{pb}}{|\mathbf{n}_{pb}|} \cdot \mathbf{d}_{pb}\right) \frac{\mathbf{n}_{pb}}{|\mathbf{n}_{pb}|} - \mathbf{d}_{pb}.$$

Note that $\mathbf{t}_b = \mathbf{d}_{p'p}$ in Fig. 1b.

Substituting (5), (7), (8), and (9) in (3), and assuming a constant approximation of ϕ_p and $\nabla\phi_p$ on a cell Ω_p in the left hand side of (3), we have the final spatial discretization:

$$\frac{|\Omega_p|}{|\nabla\phi_p|_\varepsilon} \frac{d}{dt}\phi_p = \sum_{f \in F_p} c_f(\phi_q - \phi_p + \nabla\phi_f \cdot \mathbf{t}_f) + \sum_{b \in B_p} c_b(\phi_b - \phi_p + \nabla\phi_p \cdot \mathbf{t}_b). \tag{10}$$

2.2 Iterative Nonlinear Crank-Nicolson Method

Let us denote a time step as Δt, and $\phi_p^n \approx \phi(\mathbf{x}_p, n\Delta t)$, $p \in I$, and $n \in \mathbb{N}$. The values given by the initial condition in (2) are denoted by $\phi^0 = (\phi_1^0, \ldots, \phi_{|I|}^0)^{\mathrm{T}}$. To compute ϕ^n, we use a nonlinear Crank-Nicolson method with a deferred correction method [2]. For $n \geq 1$ and $k \geq 1$, the method to solve (10) is presented:

$$\begin{aligned}\frac{|\Omega_p|}{\Delta t}\left(\phi_p^{n,k} - \phi_p^{n-1}\right) = {} & \frac{1}{2}\sum_{f \in F_p} \alpha_{pf}^{n,k-1}\left(\phi_q^{n,k} - \phi_p^{n,k} + \nabla\phi_f^{n,k-1}\cdot\mathbf{t}_f\right)\\ & + \frac{1}{2}\sum_{b\in B_p}\alpha_{pb}^{n,k-1}\left(\phi_b^{n} - \phi_p^{n,k} + \nabla\phi_p^{n,k-1}\cdot\mathbf{t}_b\right)\\ & + \frac{1}{2}\sum_{f \in F_p}\alpha_{pf}^{n-1}\left(\phi_q^{n-1} - \phi_p^{n-1} + \nabla\phi_f^{n-1}\cdot\mathbf{t}_f\right)\\ & + \frac{1}{2}\sum_{b\in B_p}\alpha_{pb}^{n-1}\left(\phi_b^{n-1} - \phi_p^{n-1} + \nabla\phi_p^{n-1}\cdot\mathbf{t}_b\right),\end{aligned} \tag{11}$$

where $\alpha_{pf}^{n,k-1} \equiv c_f^{n,k-1}|\nabla\phi_p^{n,k-1}|_\varepsilon$ and $\alpha_{pf}^{n-1} \equiv c_f^{n-1}|\nabla\phi_p^{n-1}|_\varepsilon$, for $f \in F_p \cup B_p$. Note that $\nabla\phi_p^{n,k-1} \equiv L_p(\phi_p^{n,k-1}, \phi_b^n)$ and $\nabla\phi_p^{n-1} \equiv L_p(\phi_p^{n-1}, \phi_b^{n-1})$. Moreover, for $k = 0$ the values are determined from the previous time step, e.g., $\alpha_{pf}^{n,0} = \alpha_{pf}^{n-1}$. For each n and k, one has to solve a system (11) of linear algebraic equations, where the elements of the matrix for the system can change with each n and k. Note that the original nonlinear Crank-Nicolson method [1] should use the terms $\nabla\phi_f^{n,k}\cdot\mathbf{t}_f$ and $\nabla\phi_b^{n,k}\cdot\mathbf{t}_b$ in (11) instead of $\nabla\phi_f^{n,k-1}\cdot\mathbf{t}_f$ and $\nabla\phi_b^{n,k-1}\cdot\mathbf{t}_b$, respectively. However, using the original form brings computational difficulties in general when practical industrial problems are solved because of a larger number of non-zero coefficients in the matrix and a larger communication cost for parallel computing. Therefore, the iterative deferred correction method is used in (11).

Rewriting (11) formally as a matrix equation $\mathbf{A}^{n,k-1}\phi^{n,k} = \mathbf{F}(\phi^{n,k-1})$, the k^{th} iteration is stopped at the smallest K_n such that a residual error is smaller than a chosen error bound η:

$$\frac{1}{|I|}\sum_{p\in I}\left|\left(\mathbf{A}^{n,K_n}\phi^{n,K_n} - \mathbf{F}(\phi^{n,K_n})\right)_p\right| < \eta. \tag{12}$$

Then, we define $\phi^n \equiv \phi^{n,K_n}$.

3 Numerical Experiments

Two exact solutions of the mean curvature flow equation are used in order to check the experimental order of convergence (*EOC*) of proposed algorithm (11). The numerical solutions are computed for two domains using polyhedral meshes generated by `AVL FIRE`™ in Fig. 2. For all examples in this paper, we use the threshold $\eta = 10^{-10}$ in (12) to stop the iteration. Moreover, we stop the iterations if $k > 100$ in (11). The *EOC* is computed by using an average discretization size,

$$h = \frac{1}{|I|} \sum_{p \in I} |\Omega_p|^{1/3}, \tag{13}$$

and four meshes for which h is decreasing. In Fig. 2, the polyhedral mesh in the cube domain Ω_1 is shown with $h = 1.90 \times 10^{-1}$ and we use the related finer meshes with the average discretization sizes $h = 9.52 \times 10^{-2}$, 4.76×10^{-2}, and 2.48×10^{-2}. The polyhedral mesh in the domain Ω_2 of more complex shape has $h = 6.64 \times 10^{-2}$ and the related finer meshes have $h = 4.17 \times 10^{-2}$, 2.27×10^{-2}, and 1.29×10^{-2}. Four types of the norms are used to compute the *EOC*. The errors E^2 and E^∞ are the $L^2((0, T) \times \Omega)$ and $L^\infty(0, T; L^2(\Omega))$ norms of the difference between the exact and the numerical solutions, respectively. The errors G^2 and G^∞ are the $L^2((0, T) \times \Omega)^3$ and $L^\infty(0, T; L^2(\Omega)^3)$ norms of the difference between the gradient of the exact and the numerical solutions, respectively.

The two exact solutions of (1) for $\varepsilon = 0$ on the domains in Fig. 2 are used:

$$\phi^i(\mathbf{x}, t) = \left(\frac{|\mathbf{x}|^2}{4} + t \right)^{i/2}, \tag{14}$$

where $(\mathbf{x}, t) \in \Omega_i \times [0, T]$, $i = 1, 2$, and $T = 0.16$. Note that the regularization parameter in (11) is chosen as $\varepsilon = h^2$. The functions ϕ_0 and ϕ_b in the initial and boundary conditions are obtained from the given exact solution.

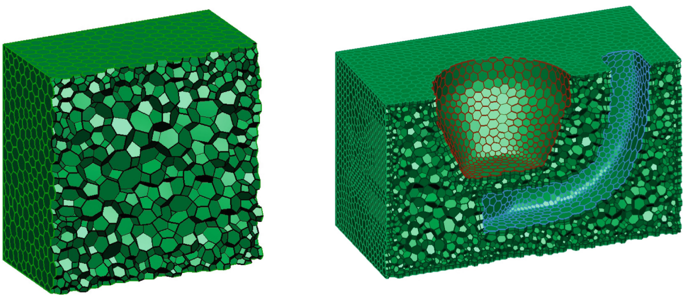

Fig. 2 A half cut view of polyhedral meshes in a cube domain $\Omega_1 = [-1.25, 1.25]^3 \subset \mathbb{R}^3$ (left) and in a domain Ω_2 of a complex shape (right)

Table 1 The *EOC* of numerical solution of (1) using the exact solution in (14) with $i = 1$ on Ω_1 (top) and Ω_2 (bottom) is presented by using the iterative nonlinear Crank-Nicolson method (11)

N	E^2	EOC	E^∞	EOC	G^2	EOC	G^∞	EOC
1	3.54×10^{-3}		9.41×10^{-3}		2.36×10^{-2}		6.60×10^{-2}	
2	7.39×10^{-4}	3.36	2.15×10^{-3}	3.17	9.58×10^{-3}	1.93	3.00×10^{-2}	1.69
3	2.08×10^{-4}	2.09	7.59×10^{-4}	1.72	4.46×10^{-3}	1.26	1.72×10^{-2}	0.92
4	4.70×10^{-5}	2.64	2.35×10^{-4}	2.08	1.86×10^{-3}	1.55	8.24×10^{-3}	1.30
N	E^2	EOC	E^∞	EOC	G^2	EOC	G^∞	EOC
1	7.03×10^{-4}		2.01×10^{-3}		1.03×10^{-2}		3.61×10^{-2}	
2	2.30×10^{-4}	2.40	8.58×10^{-4}	1.82	4.92×10^{-3}	1.59	2.21×10^{-2}	1.05
3	5.43×10^{-5}	2.38	3.49×10^{-4}	1.49	2.05×10^{-3}	1.45	1.22×10^{-2}	0.98
4	1.73×10^{-5}	2.03	1.44×10^{-4}	1.56	9.67×10^{-4}	1.33	7.19×10^{-3}	0.93

Table 2 The *EOC* of numerical solution of (14) with $i = 2$ on Ω_1 (top) and Ω_2 (bottom) is presented by using the iterative nonlinear Crank-Nicolson method (11)

N	E^2	EOC	E^∞	EOC	G^2	EOC	G^∞	EOC
1	5.02×10^{-3}		1.49×10^{-2}		4.79×10^{-2}		1.24×10^{-1}	
2	1.06×10^{-3}	3.33	2.81×10^{-3}	3.57	1.88×10^{-2}	2.01	4.99×10^{-2}	1.94
3	3.01×10^{-4}	2.08	8.94×10^{-4}	1.89	7.73×10^{-3}	1.46	2.26×10^{-2}	1.31
4	8.60×10^{-5}	2.22	2.74×10^{-4}	2.09	3.15×10^{-3}	1.59	9.85×10^{-3}	1.47
N	E^2	EOC	E^∞	EOC	G^2	EOC	G^∞	EOC
1	9.72×10^{-4}		2.58×10^{-3}		1.41×10^{-2}		3.92×10^{-2}	
2	2.91×10^{-4}	2.58	8.03×10^{-4}	2.51	6.68×10^{-3}	1.59	2.02×10^{-2}	1.42
3	6.08×10^{-5}	2.59	1.79×10^{-4}	2.48	2.46×10^{-3}	1.65	7.99×10^{-3}	1.53
4	2.10×10^{-5}	1.88	6.64×10^{-5}	1.76	1.15×10^{-3}	1.35	3.83×10^{-3}	1.30

In Tables 1 and 2, the EOC of numerical solutions of (14) with $i = 1$ and $i = 2$ are presented, respectively. We choose the time step $\Delta t = T/2^{N-1}$ for $N \in \{1, 2, 3, 4\}$, where $N = 1$ for the coarsest mesh and $N = 4$ for the finest mesh. The iterative nonlinear Crank-Nicolson method (11) shows $EOC \simeq 2$ in the error norms E^2 and E^∞ on Ω_1 and the EOC is larger than 1 in the error norms G^2 and G^∞. Note that in the case of domain Ω_2, the EOC is partially influenced by the nontrivial task of approximating the curved shape of $\partial\Omega_2$ with polyhedral meshes.

4 Conclusion

We present a cell-centered finite volume method for the regularized mean curvature flow equation, which is suitable on polyhedral meshes. The numerical experiments for the chosen examples indicate a convergence rate of around 2. Consequently, the proposed method can use the time step proportional to the average discretization size to obtain the second order accurate method in time and space.

Acknowledgements The work was supported by grants VEGA 1/0709/19 and 1/0436/20 and APVV-0522-15.

References

1. Balažovjech, M., Mikula, K.: A higher order scheme for a tangentially stabilized plane curve shortening flow with a driving force. SIAM J. Sci. Comp. **33**(5), 2277–2294 (2011)
2. Böhmer, K., Hemker, P.W., Stetter, H.J.: The defect correction approach. In: Defect Correction Methods, pp. 1–32. Springer (1984)
3. Deckelnick, K., Dziuk, G.: Error estimates for a semi-implicit fully discrete finite element scheme for the mean curvature flow of graphs. Interface Free Bound. **2**, 341–359 (2000)
4. Demirdžić, I.: On the discretization of the diffusion term in finite-volume continuum mechanics. Num. Heat Tr. B-Fund. **68**, 1–10 (2015)
5. Demirdžić, I., Muzaferija, S.: Numerical method for coupled fluid flow, heat transfer and stress analysis using unstructured moving meshes with cells of arbitrary topology. Comp. Meth. Appl. Mech. Eng. **125**, 235–255 (1995)
6. Evans, L.C., Spruck, J.: Motion of level sets by mean curvature. I. J. Differential Geom. **33**, 635–681 (1991)
7. Eymard, R., Handlovičová, A., Mikula, K.: Study of a finite volume scheme for the regularized mean curvature flow level set equation. IMA J. Numer. Anal. **31**, 813–846 (2011)
8. Gibou, F., Fedkiw, R., Osher, S.: A review of level-set methods and some recent applications. J. Comput. Phys. **353**, 82–109 (2018)
9. Hahn, J., Mikula, K., Frolkovič, P., Medl'a, M., Basara, B.: Iterative inflow-implicit outflow-explicit finite volume scheme for level-set equations on polyhedron meshes. Comp. Math. Appl. **77**, 1639–1654 (2019)
10. Hahn, J., Mikula, K., Frolkovič, P., Basara, B.: Inflow-based gradient finite volume method for a propagation in a normal direction in a polyhedron mesh. J. Sci. Comp. **72**, 442–465 (2017)
11. Handlovičová, A., Mikula, K., Sgallari, F.: Semi-implicit complementary volume scheme for solving level set like equations in image processing and curve evolution. Numeri. Math. **93**, 675–695 (2003)

12. Jasak, H.: Error analysis and estimation for the finite volume method with applications to fluid flows. Ph.D. thesis (1996)
13. Oberman, A.M.: A convergent monotone difference scheme for motion of level sets by mean curvature. Numer. Math. **99**, 365–379 (2004)
14. Osher, S., Fedkiw, R.: Level Set Methods and Dynamic Implicit Surfaces. Springer, Berlin (2000)
15. Osher, S., Sethian, J.A.: Fronts propagating with curvature dependent speed: algorithms based on Hamilton-Jacobi formulations. J. Comput. Phys. **79**, 12–49 (1988)
16. Peters, N.: Turbulent Combustion. Cambridge Monographs on Mechanics. Cambridge University Press (2000)
17. Sethian, J.A.: Level Set Methods and Fast Marching Methods, Evolving Interfaces in Computational Geometry, Fluid Mechanics, Computer Vision, and Materials Science. Cambridge University Press, New York (1999)
18. Smereka, P.: Semi-implicit level set methods for curvature and surface diffusion motion. J. Sci. Comput. **19**, 439–456 (2003)
19. Walkington, N.J.: Algorithms for computing motion by mean curvature. SIAM J. Numer. Anal. **33**, 2215–2238 (1996)